Unified Energy-Forming Framework for MMCs: Seamless GFL/GFM Transition via Internal Energy

Jeehoon Lee
School of Electrical and Electronic Engineering
Yonsei University
Seoul, South Korea
jeehun87@yonsei.ac.kr

Kyeon Hur
School of Electrical and Electronic Engineering
Yonsei University
Seoul, South Korea
khur@yonsei.ac.kr
(Corresponding author)

***Abstract*—This paper proposes a *Unified Energy-Forming Framework* for modular multilevel converters (MMCs) that enables seamless and self-adaptive transitions among grid-following (GFL), dual-port grid-forming (GFM), and stand-alone GFM modes. Conventional dual-port GFM schemes passively balance internal energy and exhibit limited adaptability to grid-strength variations. The proposed framework redefines MMC control from an energy-based perspective by integrating flexible synthetic-capacitance (FSC) regulation and energy-based seamless transition through online short-circuit ratio (SCR)-aware mode coordination within a unified structure. Through these functions, the MMC actively utilizes its internal energy to stabilize coupled AC/DC dynamics and automatically adjusts to grid-strength changes without external communication. RTDS-based electromagnetic transient (EMT) simulations on a multi-terminal high-voltage direct current (MTDC) test system demonstrate stable operation, seamless transitions, and enhanced dynamic stiffness and stability across varying grid conditions.**

***Index Terms*—Modular multilevel converter (MMC), dual-port grid-forming (GFM), energy-forming control, seamless transition**

I. INTRODUCTION

The increasing penetration of inverter-based resources (IBRs) and multi-terminal high-voltage direct current (MTDC) networks is transforming modern power systems into low-inertia hybrid AC/DC grids [1], [2]. Among various converter topologies, the modular multilevel converter (MMC) has emerged as a key enabling technology owing to its scalability and distributed energy storage capabilities [3]–[5].

Recent advances in dual-port grid-forming (GFM) control have enabled MMCs to achieve self-synchronization and stable operation under weak-grid conditions [6], [7]. However, most existing schemes passively balance internal energy rather than actively utilizing it to enhance dynamic frequency and voltage regulation. Additionally, capacitance-adaptive methods [3] are often not integrated into grid-forming control. Consequently, the converter's internal energy remains a balancing variable rather than a control input [4], [5], limiting effective AC/DC coordination.

In practical hybrid AC/DC grids, varying grid strength and loading conditions require converters to flexibly operate in grid-following (GFL), dual-port GFM, or stand-alone GFM modes [8], [9]. GFL converters may suffer from instability in weak grids, whereas GFM operation can be overly conservative or limited by available headroom in strong grids [8], [10], [11]. Therefore, a seamless and adaptive transition between these operating modes is essential to ensure operational stability and efficiency across varying grid conditions.

Furthermore, conventional dual-port GFM schemes often lack adaptability to short-circuit ratio (SCR) changes, limiting robust operation under realistic grid-strength variations. Existing seamless-transition strategies typically focus on single-port converters and do not adequately address the simultaneous AC/DC coordination required in dual-port MMCs. Moreover, most online SCR estimation methods remain supervisory and decoupled from internal energy control [12]. These limitations call for a unified control structure that tightly links internal-energy dynamics, synchronization mechanisms, and grid-strength awareness within a single energy-forming hierarchy.

This paper proposes a unified energy-forming framework that treats the MMC internal energy as a dynamic control variable, inherently linking AC frequency regulation, DC voltage dynamics, and grid-strength adaptation. By integrating flexible synthetic-capacitance (FSC) regulation, energy-based seamless transition, and online SCR-aware coordination, the proposed framework enables real-time mode adaptation and stable, continuous operation across a wide range of grid conditions.

The main contributions of this work are summarized as follows:

- **Unified energy-based coordination:** The MMC internal energy is explicitly utilized as a unifying control variable that links AC frequency and DC voltage regulation, enabling balanced and adaptive energy exchange between the two ports.
- **Seamless and adaptive operation:** A unified control framework enables smooth transitions among GFL, dual-port GFM, and stand-alone GFM modes by embedding real-time SCR awareness and adaptive synchronization within the energy-forming control hierarchy.

Validation is performed via RTDS-based electromagnetic transient (EMT) simulations of a three-terminal system designed to reflect the representative AC characteristics of the West Coast DC-highway interconnection in South Korea.

979-8-3315-8138-1

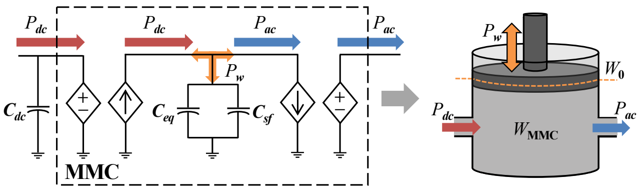

Fig. 1. Conceptual representation of stored energy in the MMC.

II. MMC Energy Control and Dual-Port GFM Fundamentals

A. Energy Dynamics of MMC

The MMC regulates AC terminal voltage and DC link voltage through independent inner loops, but it also possesses a common internal energy state W_{MMC}, representing the total energy stored in all submodule capacitors.

Each submodule contains a capacitor C_{SM} with an average voltage v_{SM}. The energy of one arm is defined as

$$W_{\text{arm}} = \tfrac{1}{2} N_{\text{SM}} C_{\text{SM}} v_{\text{SM}}^2, \tag{1}$$

where N_{SM} denotes the number of submodules per arm. For a three-phase MMC, there are six arms, so the total stored energy is the sum of the energy in all six arms. Under the approximation that the average submodule voltage is related to the DC terminal voltage by $v_{\text{SM}} \approx \frac{V_{\text{DC}}}{N_{\text{SM}}}$, the total stored energy is approximated by:

$$W_{\text{MMC}} = 3 \times 2 \times \tfrac{1}{2} N_{\text{SM}} C_{\text{SM}} v_{\text{SM}}^2 = \tfrac{1}{2} C_{\text{eq}} V_{\text{DC}}^2, \tag{2}$$

where the equivalent capacitance is defined as

$$C_{\text{eq}} = \frac{6C_{\text{SM}}}{N_{\text{SM}}}. \tag{3}$$

Equations (2)–(3) provide a direct physical link between the converter's stored energy and the average capacitor voltage, which governs its dynamic stiffness in response to AC–DC power imbalance.

The instantaneous energy variation satisfies the fundamental power–energy relation

$$\dot{W}_{\text{MMC}} = P_{dc} - P_{ac}, \tag{4}$$

where P_{ac} and P_{dc} denote the instantaneous AC and DC powers, respectively. When $P_{ac} = P_{dc}$, W_{MMC} remains constant; otherwise, its deviation represents the net energy exchange between the two ports.

Figure 1 illustrates a conceptual representation of the stored energy in the MMC. The internal energy W_{MMC} can be viewed as a reservoir that absorbs or releases energy depending on the instantaneous imbalance between P_{ac} and P_{dc}. This reservoir mediates energy transfer between the AC and DC terminals in both steady-state and transient conditions.

Energy-based control redefines W_{MMC} from a passive state requiring stabilization into an active coordination variable that governs system-wide dynamics. By explicitly shaping the trajectory of W_{MMC}, the control scheme simultaneously helps regulate AC frequency and DC voltage, effectively unifying the two ports through a single, energy-coherent control law.

B. Energy–Frequency and Energy–Voltage Coupling in Dual-Port GFM

In the dual-port grid-forming concept [6], the internal energy W_{MMC} serves as a common state variable that inherently couples the AC and DC terminals. The stored energy varies according to the instantaneous power imbalance, as expressed in (4). This fundamental relation links the internal energy to both the AC frequency and DC voltage through the following energy-based droop laws:

$$\omega^* = \omega_0 + k_\omega^{\text{ac}} (W_{\text{MMC}} - W_0), \tag{5}$$

$$V_{\text{DC}}^* = V_{\text{DC},0} + k_v^{\text{dc}} (W_{\text{MMC}} - W_0). \tag{6}$$

Here, ω_0 and $V_{\text{DC},0}$ denote the nominal references, W_0 is the steady-state internal energy, and k_ω^{ac} and k_v^{dc} are proportional gains defining the sensitivity of frequency and DC voltage to internal energy deviation.

When W_{MMC} increases, indicating an excess of stored energy, both ω^* and V_{DC}^* rise to drive power export toward the AC and DC networks. Conversely, when W_{MMC} decreases, these references fall, drawing power import until equilibrium is restored. This direct coupling among internal energy, frequency, and DC voltage enables the converter to form both AC and DC voltages simultaneously, achieving self-synchronization and long-term power balance without external synchronization or coordination.

The internal energy W_{MMC} thus functions as a unified buffer that provides virtual inertia for AC stability and synthetic capacitance for DC voltage regulation. Conventional approaches rely on fixed AC–DC coupling coefficients, which limit stability margins due to the limited intrinsic energy storage of MMCs (approximately 30–60 ms). The proposed framework addresses this limitation through an active energy-shaping mechanism, as detailed in Section III.

III. Proposed Unified Energy-Forming Framework

A. Concept and Unified Control Architecture

The proposed Unified Energy-Forming Framework extends the dual-port GFM principle into an energy-oriented control hierarchy integrating internal energy regulation, adaptive synchronization, and grid-condition awareness. Figure 2 shows the overall architecture, built upon an energy-based dual-port GFM controller with AC–DC decoupled control. Four coordinated functions enable self-adaptive operation across varying grid conditions.

The first function, the FSC control, shapes W_{MMC} to synthesize an adjustable effective capacitance, enhancing DC voltage stiffness while providing inertia-like support to the AC side. The second function enables a seamless GFL transition by emulating PLL-type synchronization; under strong-grid conditions, the converter follows the grid phase, realizing AC-following/DC-forming operation. Conversely, the third function governs the seamless GFM transition, where the DC voltage becomes the regulating variable under weak-grid conditions, establishing DC-following/AC-forming control. Finally, an online SCR estimator with mode-coordination

979-8-3315-8138-1

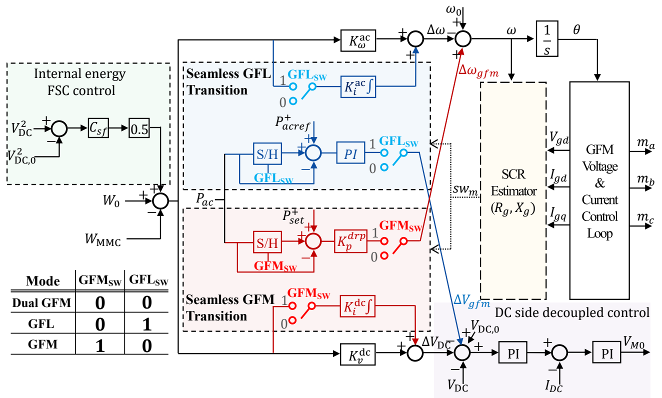

Fig. 2. Overall control structure of the proposed Unified Energy-Forming Framework.

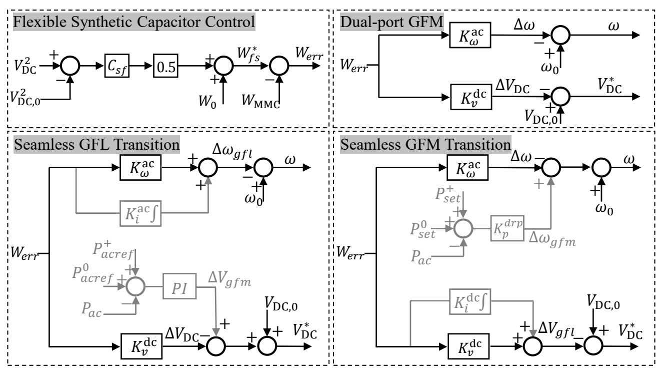

Fig. 3. Energy-based FSC and seamless transition control.

logic continuously monitors grid impedance and autonomously determines the appropriate operating mode among GFL, dual-port GFM, and stand-alone GFM. The SCR estimator operates at a supervisory time scale of 100 ms, slower than the inner current and voltage control loops. A mode transition is triggered only after consistent SCR estimates are observed for ten consecutive updates (1 s) to avoid chattering.

Together, these coordinated functions constitute an energy-coherent control paradigm that allows the MMC to adapt smoothly between grid-following and grid-forming behaviors.

B. Energy-Based FSC Control and Seamless Transition

The energy-forming framework centers on how the converter's energy reference is generated and adaptively regulated.

1) FSC Control: As shown in Fig. 3, the FSC modifies the conventional fixed energy reference so that it varies dynamically with the converter's operating state, thereby improving disturbance response and AC/DC coupling.

The synthetic energy reference W_{sf}^* is defined as

$$W_{sf}^* = \tfrac{1}{2}C_{sf}\left(V_{\mathrm{DC}}^2 - V_{\mathrm{DC},0}^2\right) + W_0, \tag{7}$$

where V_{DC} is the measured DC-terminal voltage, $V_{\mathrm{DC},0}$ is the nominal reference, and W_0 denotes the steady-state internal energy reference.

The synthetic capacitance C_{sf} is given by

$$C_{sf} = k_{sf}C_{\mathrm{eq}} = 6k_{sf}\frac{C_{\mathrm{SM}}}{N_{\mathrm{SM}}}, \tag{8}$$

where k_{sf} is an adaptive gain that determines the effective-capacitance contribution. By tuning k_{sf}, the controller redistributes the energy buffer between the MMC's internal energy and the DC system, achieving coordinated inertia support and improved DC-voltage stability.

The DC side power balance becomes

$$P_{\mathrm{dc}} - P_{\mathrm{ac}} = \tfrac{1}{2}(C_{dc} + C_{sf})\,\frac{dV_{\mathrm{DC}}^2}{dt}, \tag{9}$$

which shows that the FSC effectively increases the DC-link capacitance by combining the physical capacitor C_{dc} with the synthetic element C_{sf}. This effectively expands the apparent energy storage and mitigates DC-voltage oscillations without additional hardware.

2) Seamless Transition Control: The seamless transition control adaptively shifts one side of the dual-port controller from proportional (P) energy balancing to proportional–integral (PI) energy tracking. By gradually converting the steady-state error–tolerant P loop into a zero-error PI loop, the converter transitions smoothly between modes without dynamic discontinuity, as illustrated in Fig. 3.

In conventional GFL operation, a phase-locked loop (PLL) aligns the converter phase by forcing the q-axis voltage to zero in the dq frame. Similarly, in the proposed energy-based scheme, the GFL transition is achieved by driving the internal energy error W_{err} to zero through a PI-controlled frequency correction:

$$\Delta\omega_{\mathrm{gfl}} = k_\omega^{\mathrm{ac}}W_{\mathrm{err}} + k_i^{\mathrm{ac}}\int W_{\mathrm{err}}\,dt, \tag{10}$$

where k_ω^{ac} and k_i^{ac} are the proportional and integral gains. This emulates PLL behavior in the energy domain, allowing the converter phase to follow the grid frequency.

Conversely, the GFM transition regulates the DC voltage instead of frequency. The internal energy error is again forced to zero through

$$\Delta V_{\mathrm{gfl}} = k_v^{\mathrm{dc}}W_{\mathrm{err}} + k_i^{\mathrm{dc}}\int W_{\mathrm{err}}\,dt, \tag{11}$$

where k_v^{dc} and k_i^{dc} are DC side control gains. This yields a DC-following/AC-forming operation in which the converter tracks the external DC voltage while autonomously generating a stable AC waveform.

During both transitions, the forming and tracking functions operate concurrently to maintain power continuity. In the GFL transition, the phase-tracking mechanism follows the grid frequency while the DC side maintains voltage forming via ΔV_{gfm}. The active power sampled at the switching instant is held (sample-and-hold) as P_{ref}, preventing any power step. In the GFM transition, the converter tracks the DC voltage while forming the AC side through a droop-based $\Delta\omega_{\mathrm{gfm}}$. This coordinated operation preserves energy balance and ensures truly seamless transitions between GFL and GFM modes.

C. Online SCR Estimation and Adaptive Mode Coordination

To enable adaptive coordination without active perturbations, an online SCR estimation algorithm is integrated. Unlike

979-8-3315-8138-1

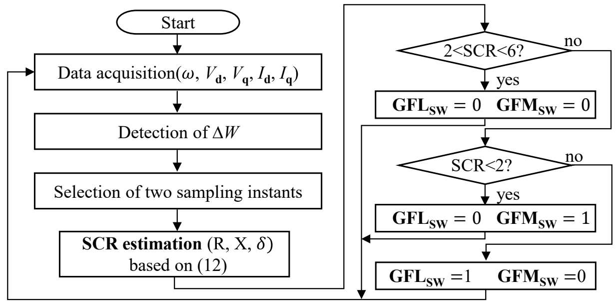

Fig. 4. Flowchart of online impedance estimation and adaptive mode coordination.

conventional injection-based methods, the proposed approach estimates the equivalent grid impedance from phase deviations inherently generated by the grid-forming (GFM) controller in response to internal energy variations. Following [12], the estimated grid impedance $\hat{\mathbf{Z}}_{\mathrm{g}}$ is obtained from two consecutive phasor measurements:

$$\hat{\mathbf{Z}}_{\mathrm{g}} = \frac{\mathbf{V}_{t0} - \mathbf{V}_{t1} e^{j\Delta\theta}}{\mathbf{I}_{t0} - \mathbf{I}_{t1} e^{j\Delta\theta}} - \mathbf{Z}_{\mathrm{T}}, \tag{12}$$

where $\mathbf{V}_{t0,t1}$ and $\mathbf{I}_{t0,t1}$ denote terminal voltage and current phasors at two sampling instants with phase deviation $\Delta\theta$, and $\mathbf{Z}_{\mathrm{T}}$ represents the transformer impedance. The resulting $\hat{\mathbf{Z}}_{\mathrm{g}} = \hat{R}_{\mathrm{g}} + j\hat{X}_{\mathrm{g}}$ provides the resistive and reactive components for SCR evaluation.

As shown in Fig. 4, the algorithm continuously evaluates grid parameters $(R_{\mathrm{g}}, X_{\mathrm{g}})$ from two sampling instants T_0 and T_1. The calculated SCR is then passed to the mode-coordination logic, which autonomously selects the appropriate operating mode (GFL, dual-GFM, or GFM).

IV. EMT-Based Validation and Case Studies

The proposed Unified Energy-Forming Framework was validated through real-time EMT simulations using the RTDS platform. A three-terminal ±300 kV, 1 GW MTDC system was modeled to reflect the general operating characteristics of the West Coast DC highway interconnection, as shown in Fig. 5. The study emulates a realistic hybrid AC/DC environment, where the southern terminal represents a renewable-dominant area controlled by the proposed algorithm, and the other two terminals correspond to a thermal generation hub (AC-GFL/DC-GFM) and a large offshore wind cluster (AC-GFM/DC-GFL), respectively. The AC grid is modeled as an equivalent frequency-forming source with constant PQ loads, such that frequency deviations arise from power imbalance and are regulated through grid-forming control. The key MMC hardware and control parameters used in the simulation are listed in Table I.

A. Scenario 1: Validation of FSC Functionality in Dual-Port Operation

To evaluate the effectiveness of the proposed FSC control under dual-port grid-forming operation, both AC and DC disturbance scenarios were tested. On the AC side, the active power demand was increased and decreased by 700 MW,

TABLE I
MMC and Control Parameters for RTDS Validation

MMC Hardware		*Control Parameters*	
N_{SM}	200	k_{sf}	0, 1, 2, 3
C_{SM} [μF]	10,000	k_{ω}^{ac}	0.5
L_{arm} [H]	0.03	k_{v}^{dc}	1.0
V_{DC} [kV]	±300	k_{i}^{ac}	0.05
S_{rated} [GW]	1.0	k_{i}^{dc}	0.05

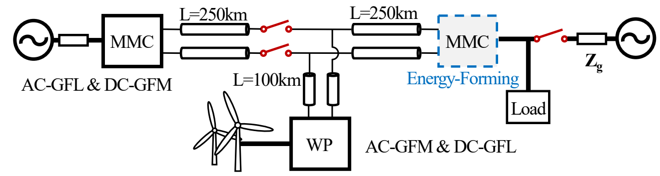

Fig. 5. RTDS-based three-terminal ±300 kV, 1 GW MTDC system.

followed by the disconnection of the AC source. On the DC side, the wind-power injection was varied by ±700 MW, after which the DC terminal associated with the thermal generation hub was tripped. Each case was simulated under two configurations: (i) without FSC ($k_{sf} = 0$) and (ii) with FSC enabled using different coefficients ($k_{sf} = 1$, 2, and 3).

Figures 6(a) and 6(b) present the dynamic responses for the AC and DC disturbance scenarios, respectively. The plotted variables include AC frequency, DC voltage, AC active power, DC active power, MMC internal active power, and the converter's stored energy. At 0.5 s and 1.5 s, step changes in active-power flow were applied, and at 2.5 s the corresponding source was disconnected. Without FSC, both the AC and DC terminals exhibited pronounced oscillations and slow recovery following each disturbance. As k_{sf} increased, the converter's dynamic stiffness improved significantly, reducing frequency and voltage deviations and suppressing oscillatory behavior. This improvement results from actively utilizing W_{MMC} to buffer power imbalance, keeping energy variations within practical margins under the considered disturbances, while fault-level events are handled by current limiting and protection mechanisms.

B. Scenario 2: Seamless Mode Transition with SCR Variation

The second case study validates the proposed online SCR estimation algorithm and the seamless automatic mode transition under varying grid strength. In this case study, SCR variation is implemented by switching parallel RL branches in the equivalent Thevenin impedance Z_g, representing grid-strength changes due to network reconfiguration. Figures 6(c) and 6(d) illustrate the dynamic responses for decreasing and increasing SCR conditions, corresponding to the transitions toward GFM and GFL operation, respectively. The system initially operated in dual-port GFM mode with an SCR of 4. At 0.5 s, the grid strength was varied, first decreased to 1.5 and later increased to 6.5, causing small internal-energy and power fluctuations that activated the SCR estimation algorithm. When the estimated SCR crossed the predefined threshold, the controller autonomously transitioned to the corresponding operating mode after a 1.0 s delay.

979-8-3315-8138-1

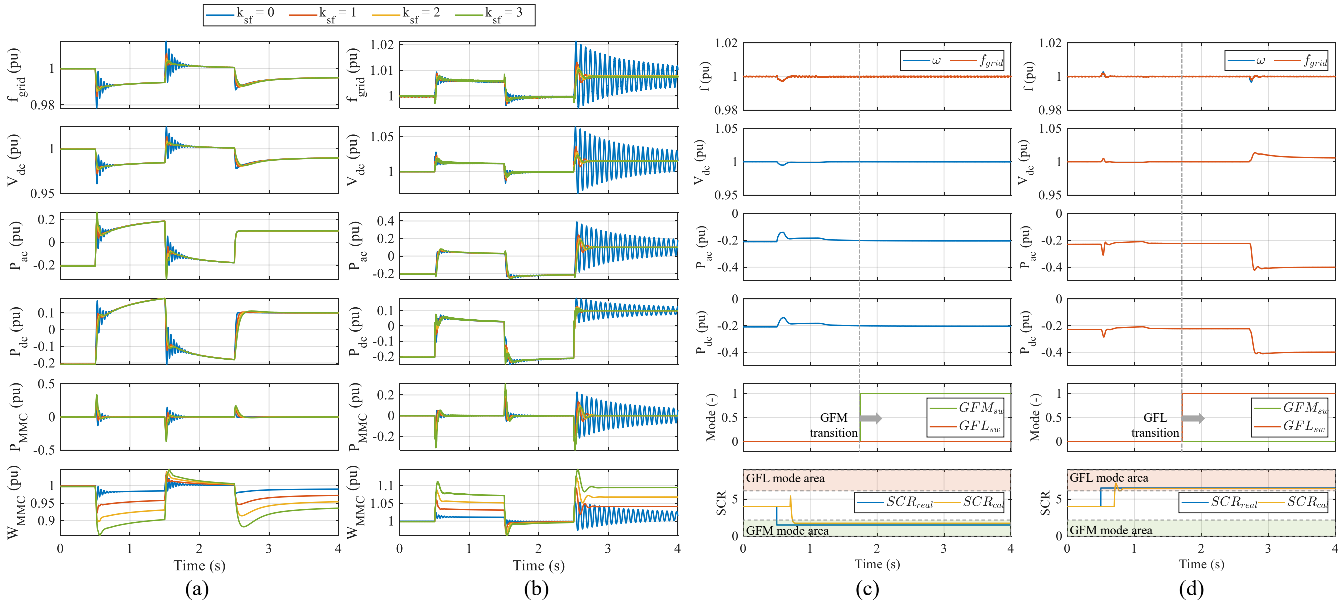

Fig. 6. RTDS-based validation results of the proposed Unified Energy-Forming Framework: (a) AC disturbance scenario, (b) DC disturbance scenario, (c) SCR reduction leading to seamless GFM transition, and (d) SCR recovery leading to seamless GFL transition and active power regulation.

During SCR reduction, the converter transitioned smoothly from dual-port operation toward AC-side grid-forming behavior while maintaining stable frequency and DC voltage. When the SCR increased, the converter adopted AC-side grid-following behavior, transferring surplus renewable power from the AC grid to the DC network by regulating the active power to -0.4 p.u. Throughout both transitions, the AC frequency, DC voltage, and active power remained continuous and well regulated, confirming that the proposed seamless control strategy ensures stable and disturbance-free power exchange across varying grid conditions.

V. Conclusion

A Unified Energy-Forming Framework for MMCs has been presented, enabling seamless transitions among GFL, dual-port GFM, and GFM operations through internal energy regulation, synthetic-capacitance control, and adaptive SCR-based coordination. The proposed framework redefines converter operation from a mode-based to an energy-coherent perspective, achieving self-synchronized AC/DC control without external communication. RTDS simulations on a ± 300 kV, 1 GW three-terminal MTDC test system verified stable and continuous operation across a wide range of grid strengths, demonstrating its capability to unify frequency, voltage, and energy control within a single structure. This framework paves the way for scalable, adaptive MMC control strategies applicable to future large-scale MTDC grids and renewable-dominant hybrid networks.

References

[1] Y. Zhang, X. Liu, and L. Xu, "A comprehensive review of modular multilevel converter control strategies for hvdc and mtdc systems," *IEEE Transactions on Power Delivery*, vol. 36, no. 3, pp. 1583–1602, 2021.

[2] E. Sánchez-Sánchez, E. Prieto-Araujo, and O. Gomis-Bellmunt, "Energy-based control of modular multilevel converters for grid-forming applications," *IEEE Journal of Emerging and Selected Topics in Power Electronics*, vol. 8, no. 2, pp. 1477–1490, 2020.

[3] K. Shinoda, A. Benchaib, J. Dai, and X. Guillaud, "Virtual capacitor control: Mitigation of dc voltage fluctuations in mmc-based hvdc systems," *IEEE Transactions on Power Delivery*, vol. 33, no. 1, pp. 455–466, 2018.

[4] H. Kim, J. Kang, J. W. Shim, J. Beerten, D. Van Hertem, H.-J. Jung, C.-K. Kim, and K. Hur, "Exploiting redundant energy of mmc–hvdc to enhance frequency response of low-inertia ac grid," *IEEE Access*, vol. 7, pp. 157 876–157 887, 2019.

[5] R. Yang, G. Shi, C. Zhang, G. Li, and X. Cai, "Internal energy-based grid-forming control for mmc-hvdc systems with wind farm integration," *IEEE Transactions on Industry Applications*, vol. 59, no. 1, pp. 503–512, 2023.

[6] D. Groß, E. Sánchez-Sánchez, E. Prieto-Araujo, and O. Gomis-Bellmunt, "Dual-port grid-forming control of mmcs and its applications to grids of grids," *IEEE Transactions on Power Delivery*, vol. 37, no. 6, pp. 4721–4735, 2022.

[7] J. Arévalo-Soler, M. Nahalparvari, D. Groß, E. Prieto-Araujo, S. Norrga, and O. Gomis-Bellmunt, "Small-signal stability and hardware validation of dual-port grid-forming interconnecting power converters in hybrid ac/dc grids," *IEEE Journal of Emerging and Selected Topics in Power Electronics*, vol. 13, no. 1, pp. 809–822, 2025.

[8] X. Gao, D. Zhou, A. Anvari-Moghaddam, and F. Blaabjerg, "Seamless switching method between grid-following and grid-forming control for renewable energy conversion systems," *IEEE Transactions on Industry Applications*, vol. 60, no. 5, pp. 7192–7204, 2024.

[9] I. Lorzadeh, O. Lorzadeh, D. V. Bozalakov, L. Dupré, and L. Vandevelde, "Unified hybrid control framework integrating grid-forming and grid-following capabilities in a single vsi under islanded conditions," *IEEE Access*, vol. 12, pp. 1160–1174, 2024.

[10] Z. Liu, L. Zhang, and Z. Hu, "An adaptive multi-mode switching control strategy to improve the stability of virtual synchronous generator with wide power grid strength variation," *IET Generation, Transmission & Distribution*, vol. 16, no. 2, pp. 307–323, 2022.

[11] D. B. Rathnayake, P. Hu, and J. Fletcher, "Grid-forming inverter modeling, control, and applications: A review," *IEEE Access*, vol. 9, pp. 114 781–114 807, 2021.

[12] J. Yu, W. Liu, J. Sun, F. Zhang, and Y. Yang, "An improved grid impedance estimator for grid-forming converters in consideration of controller dynamics," *International Journal of Electrical Power & Energy Systems*, vol. 154, p. 109424, 2023.

979-8-3315-8138-1